JOURNAL OF CATALYSIS 127, 698–705 (1991)

Structural and Kinetic Studies in Propene Oxidation over Sb Oxide Dispersed on TiO_2

TAKEHIKO ONO,* MASARU KIRYU,* MASAHARU KOMIYAMA,† AND ROBERT L. KUCZKOWSKI‡

*Department of Applied Chemistry, University of Osaka Prefecture, Sakai, Osaka 591, Japan, †Department of Chemistry, Faculty of Liberal Arts and Education, Yamanashi University, Kofu, Yamanashi 400, Japan, and ‡Department of Chemistry, University of Michigan, Ann Arbor, Michigan 48109

Received February 13, 1990; revised August 20, 1990

Antimony oxide dispersed on TiO_2 was characterized using FTIR, Raman, and Auger spectroscopies as well as XRD. They indicate that the electronic environment about Sb is perturbed at low concentration suggesting that the structure of Sb oxide on TiO_2 is somewhat distorted as compared to Sb_6O_{13}. The oxidation of labeled propene such as CH_2=CH—CD_3, $^{13}CH_2$=CH—CH_3, and *cis*-CHD=CD—CH_3 was examined on Sb_6O_{13} and Sb–Ti oxide catalysts. The results indicate that the first hydrogen abstraction is rate determining and that there is little or no isotope effect in the second hydrogen abstraction over Sb and Sb–Ti oxide catalysts. The oxidation kinetics was discussed on the basis of a modified redox mechanism. The reduction step was promoted by a factor of ca. 50 over Sb oxide dispersed on TiO_2 as compared to that on unsupported Sb_6O_{13}. Rate promotion was mainly attributed to the increase in the amount of active sites for the reduction step. © 1991 Academic Press, Inc.

INTRODUCTION

Several mixed oxides containing Sb oxide are active catalysts for the partial oxidation and ammoxidation of olefins (*1, 2*). Regarding U–Sb oxide catalysts, Grasselli *et al.* (*3*) have proposed that Sb^{3+}–O–Sb^{5+} and Sb^{5+}–O–Sb^{5+} moieties are responsible for π-allyl formation and oxygen insertion in acrolein formation, respectively. Volta *et al.* (*4*) have proposed that the surface Sb^{3+}–Sb^{5+} couples produced on SnO_2 should be responsible for partial oxidation activity. Recently it has been proposed that the rutile structure oxides play an important role in the promotion of Sb oxide for the oxidation and ammoxidation of olefins over Sb–Sn and Sb–Fe oxide systems (*2*).

We have previously reported that there is an isotope effect in the first hydrogen abstraction and little or no isotope effect in the second hydrogen abstraction for the oxidation of propene over Sb–Sn oxide catalysts (*5, 6*). Kinetic features on this catalyst have indicated that the promotion of the oxidation reaction can be attributed to an increase in the reduction step due to the presence of Sn ions.

TiO_2 has been widely used as a support for both metal (*7*) and metal oxide (*8*) catalysts. The oxidation activity as well as structure of V oxide are strongly affected by the TiO_2 support (*8*). One of the authors has also reported that the Mo oxide and V oxide highly dispersed on TiO_2 (*9*) and ZrO_2 (*10*) have higher activities in propene oxidation than crystalline MoO_3 or V_2O_5. The promoter action was attributed to the presence of polymolybdate or polyvanadate species and the rate increase was attributed to an acceleration of the reduction step in the redox mechanism.

In this paper the activity and selectivity for propene oxidation to acrolein over Sb oxide dispersed on TiO_2 were studied in much greater detail. The oxidation of labeled propene using CH_2=CH—CD_3, *cis*—CHD=CD—CH_3, and $^{13}CH_2$=CH—CH_3

0021-9517/91 $3.00

TABLE 1

Properties of the Catalysts

Catalyst (Sb at.%)[a]	Phase identified by XRD	Specific BET surface area (m^2g^{-1})	Crystalline % of Sb_6O_{13}
TiO_2[b]	Anatase (70%) + rutile (30%)	40	
Sb(5.5)–Ti–O	TiO_2	35	0
Sb(18)–Ti–O	TiO_2, Sb_6O_{13}	33	15
Sb(55)–Ti–O	TiO_2, Sb_6O_{13}	35	84
Sb(100)	Sb_6O_{13}	28	100

[a] Antimony loading, expressed as the atomic ratio 100Sb/(Sb + Ti).
[b] Heated at 500°C for 8 hr prior to catalyst preparation.

was investigated. The oxidation kinetics was discussed on the basis of a modified redox mechanism. The structure of Sb oxide on TiO_2 was examined by means of XRD, FTIR, Raman, and Auger spectroscopy. The correlation between the structure of Sb oxide on TiO_2 and the catalytic activity is discussed.

EXPERIMENTAL

Catalyst preparation. Sb(5.5, 18, and 55 atom%)–Ti oxide catalysts were prepared as follows: $SbCl_5$ was added into aqueous slurries containing desired quantities of TiO_2 (Anatase: P-25, Degussa Co. Ltd.). The slurries were precipitated with ammonia solution and the resulting precipitates and slurries were filtered, dried, and heated at 450°C. The catalysts used are listed in Table 1. As described below, Sb_6O_{13} (Sb^{3+}/Sb^{5+} = 1/2) was formed during preparation in spite of the use of $SbCl_5$ (Sb^{5+}).

Procedure and apparatus. The catalytic oxidation of propene was carried out in a closed circulation system (ca. 300 or 1000 cm^3 in volume). The reaction products such as acrolein, CO_2, and CO were analyzed by gas chromatography. The reactants CH_2=CH—CD_3 (99%), *cis*-CHD=CD—CH_3 (96.7%), and $^{13}CH_2$=CH—CH_3 (99%) were obtained from MSD Canada, Ltd. CH_2=CH—CH_3 and O_2 were obtained from regular commercial cylinders (99%).

Microwave spectroscopy was used to determine the relative amounts of the isotopic acrolein products using a Hewlett–Packard 8460A spectrometer (located at Univ. of Michigan). The 4_{04}–3_{03}, 4_{14}–3_{13}, and 4_{13}–3_{12} transitions were mainly used. The procedure is described elsewhere (*6, 11, 12, 13*). This was not a sufficiently large set of transitions to obtain very high precision for the samples containing 3–4 isotopic species, but the precision in the isotopic ratios (±5% to ±10%) in Tables 3–5 is sufficient to provide useful insights on the reaction processes.

X-ray diffraction patterns of the catalysts were obtained on a Rigaku Denki RAD-rA diffractometer using Cu$K\alpha$ radiation. The goniometer stepper motor system and the signal were interfaced with a versatile data acquisition system. Using a step scanning method a small amount of crystalline phase is detectable. IR spectra were recorded on a Shimadzu FTIR 4000 spectrometer (located at Kobe University). The sample was prepared by mixing KBr and Sb–Ti–O oxides (ca. 1 wt%). The Raman spectra were recorded using a JASCO NR-1000 laser Raman spectrometer. An Argon ion laser was tuned to the 514.5 nm line for excitation. The X-ray-excited Auger spectra of the catalysts were recorded on a Shimazdu ESCA 750 spectrometer (located at Tohoku University) using Mg$K\alpha$ radiation.

TABLE 2

Characterization of the Catalysts

Catalyst (Sb, at.%)	Noncrystalline Sb oxide (μmol m^{-2}-TiO_2)	IR spectra of Sb oxide (cm^{-1})	Auger Sb $M_4N_{4,5}N_{4,5}$ peaks (eV)
Sb(5.5)–Ti–O	2.7	900–890	460.0
Sb(18)–Ti–O	9.8	895–870, 720	459.6
Sb(55)–Ti–O	10	870, 770	459.6
Sb_6O_{13}		870–850, 760, 560	459.6

RESULTS AND DISCUSSION

Characterization of Sb–Ti–O catalysts. XRD patterns of the Sb(5.5)–Ti–O catalyst showed only the lines due to TiO_2 (anatase + rutile). The Sb(18) and Sb(55)–Ti–O showed lines due to Sb_6O_{13}(ASTM 21-51) and TiO_2. The amount of crystalline Sb_6O_{13} in these catalysts was estimated by a comparison of the XRD intensities of Sb_6O_{13} for a physical mixture of Sb_6O_{13} and TiO_2 and the catalysts. After the amounts of crystalline Sb_6O_{13} were estimated (Table 1), the percentages of noncrystalline Sb oxide were determined as 100% for Sb(5.5)–, 85% for Sb(18)–, and 16% for Sb(55)–Ti–O. These may include very small particles (below 5 nm) of Sb_6O_{13} which could not be detected by this method. The line broadening of Sb_6O_{13} peaks in the catalysts was not observed. The amounts of noncrystalline Sb oxide determined as described above are 2.7 μmol m^{-2} for Sb(5.5)–, 9.8 for Sb(18)–, and 10 for Sb(55)–Ti–O (Table 2). The amount of Sb oxide on the surface of TiO_2 does not seem to increase above ca.10 μmol m^{-2}–TiO_2. With Sb(55)–Ti, the remaining Sb oxides crystallize as Sb_6O_{13}.

The FTIR spectra of the Sb–Ti–O catalysts are shown in Fig. 1 and their peak positions are listed in Table 2. The spectra were obtained by subtracting the TiO_2 spectra from the original spectra of the catalysts. Sb(5.5)–Ti–O has very weak bands at 900–890 cm^{-1}. Sb(18)–Ti–O catalyst has bands at 895–870 and 720 cm^{-1}. Sb(55)–Ti–O has bands at 870 and 770 cm^{-1}. The IR bands of Sb_6O_{13} were reported at 870–850, 760, and 560 cm^{-1} (*5*). Thus, the bands with Sb(18)– and Sb(55)–Ti–O are attributable to Sb_6O_{13}. Raman spectra of Sb(5.5)– and Sb(18)–Ti–O showed only TiO_2 peaks. Sb(55)–Ti–O had a peak at 850 cm^{-1} due to Sb oxide. As has been reported by Sala and Trifiro (*14*), the band around 850 cm^{-1} is attributable to the Sb=O stretching vibration. On TiO_2, this band shifts from 870 to ca. 900 cm^{-1}, going from Sb(55) to Sb(5.5). This indicates that the Sb oxide seems to be more distorted at lower Sb content on TiO_2 compared to Sb_6O_{13}. This is in contrast to the case of Mo oxide on ZrO_2 or TiO_2 (*9, 10*), where the bands of Mo=O were shifted to lower wavenumber at low Mo concentration, for example, from 970 to 930 cm^{-1}.

For analysis by Auger electron (A.e.) spectroscopy, the insulating nature of the

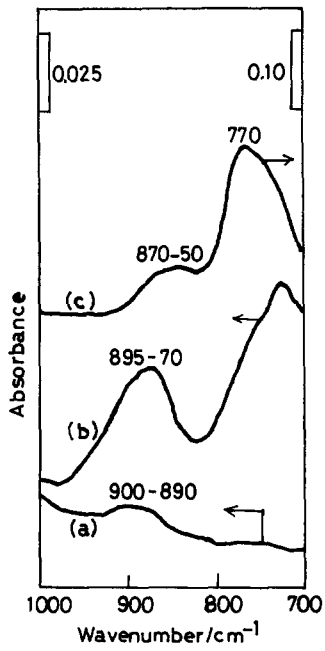

FIG. 1. FTIR spectra of SB–Ti oxide catalysts. (a) Sb(5.5)–Ti–O, (b) Sb(18)–Ti–O, and (c) Sb(55)–Ti–O. Each spectra was obtained after subtraction of the TiO_2 spectra.

Sb–Ti–O catalysts made it difficult to obtain electron-excited A.e. spectra, and we resorted to the use of X-ray excitation instead. Table 2 lists the auger peak positions obtained by using Mg$K\alpha$ irradiation. The kinetic energies of the Sb $M_4N_{4,5}N_{4,5}$ peaks are 459.6 eV for Sb_6O_{13}, Sb(18)–, and Sb(55)–Ti–O. That of Sb(5.5)–Ti–O is 460.0 eV, which is a little higher than the other catalysts. This peak shift to higher kinetic energy value reflects an increase in the Sb^{3+}/Sb^{5+} ratio in Sb oxides (*15*). The surface Sb oxide in the Sb(5.5)–Ti–O is apparently enriched with Sb^{3+} compared with the stoichiometric Sb_6O_{13} or the other samples examined here.

As described previously (*5*), the Sb–Ti oxide catalysts did not seem to have the *n*-type free electrons produced by the dissolution of Sb ions into TiO_2 lattice because the IR transmission, i.e., background, of TiO_2 did not decrease by the presence of Sb oxide. The highly insulating character of the catalysts for Auger measurements also seems to come from little or no presence of electrons in the conduction band. Zenkovets *et al.* (*16*) reported that some Sb ions are dissolved into TiO_2 lattice, whose catalysts were heated at high temperature (750°C).

Oxidation activity of Sb–Ti oxide catalysts. As shown in Fig. 2, which is obtained from our previous paper (*5*), the TiO_2 (P-25, anatase 70%) support itself has a high activity for the total oxidation of propene. Sb(18)–Ti–O is less active by a factor of ca. 10. But the selectivity to acrolein rises to 70% which is as high as that over Sb_6O_{13}. However, the activity of the Sb(18)–Ti–O catalyst is ca. 20 times higher than that of Sb_6O_{13}. The Sb(55)–Ti–O has a similar activity and acrolein selectivity as Sb (18)–Ti–O. These results indicate that the activity due to TiO_2 seems to disappear above ca. 18 at% of Sb and that the oxidation activity mainly comes from Sb oxide dispersed on it.

Labeled propene oxidation on Sb–Ti–O catalysts. In order to understand the rate

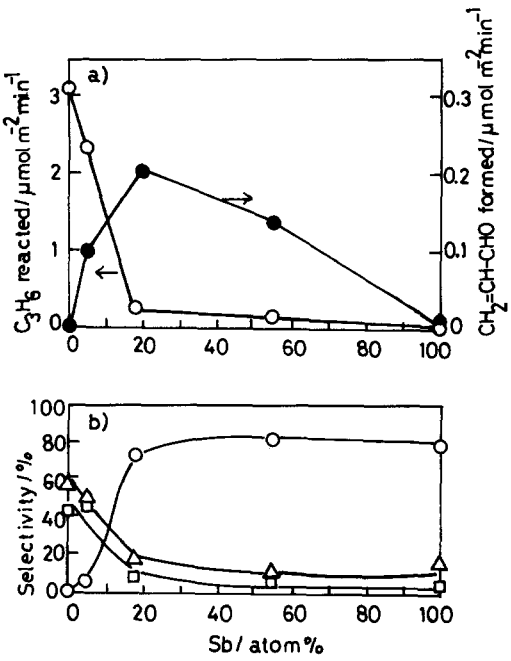

FIG. 2. (a) Rates of propene conversion over Sb–Ti oxide catalysts as a function of Sb content. $P_{C_3H_6}$ = 24 Torr, P_{O_2} = 25 Torr, and temperature = 400°C. (b) Product selectivities: (○) CH_2=CH—CHO, (□) CO, and (△) CO_2; reproduced from Ref. (*5*).

determining step, an equimolar mixture of CH_2=CH—CH_3 and CH_2=CH—CD_3 was oxidized by the catalysts. As shown in Table 3, the ratios of CH_2=CH—CHO/(CH_2=CH—CDO + CD_2=CH—CHO) were 1/0.58 with Sb_6O_{13} and 1/0.47 with the Sb (18)–Ti–O catalyst. Table 4 shows the result for the oxidation of $^{13}CH_2$=CH—CH_3 over Sb(18)–Ti–O catalyst. The ratio of $^{13}CH_2$=

TABLE 3

Relative Amounts of Acrolein Obtained from the Oxidation of CH_2=CH—CH_3 and CH_2=CH—CD_3 over Two Catalysts[a]

	CH_2=CH—CHO	CH_2=CH—CDO	CD_2=CH—CHO
Sb(18)–Ti–O	1.00	0.23	0.24
Sb_6O_{13}	1.00	0.28	0.30

[a] Experimental conditions: temperature 400°C, propene = 15 Torr, P_{O_2} = 28 Torr, propene conversion 2.4%, acrolein selectivity 71%, and CH_2=CH—CH_3 : CH_2=CH—CD_3 = 1 : 1.

TABLE 4

Relative Amounts of ^{13}C–Acrolein from Oxidation of $^{13}CH_2$=CH—CH_3 over Sb(18)–Ti–O[a]

	$^{13}CH_2$=CH—CHO	CH_2=CH—^{13}CHO
Sb(18)–Ti–O	1.00	0.90

[a] Temperature 400°C, $^{13}CH_2$=CH—CH_3 (99%) = 7.5 Torr, P_{O_2} = 30 Torr, propene conversion 8.3%, and acrolein selectivity ca. 70%.

CH—CHO/CH_2=CH—^{13}CHO is nearly one within experimental uncertainty, indicating that both terminal carbon atoms are oxidized with equal probability. Thus, the ratio of CH_2=CH—CHO/(CH_2=CH—CDO + CD_2=CH—CHO) gives the initial deuterium isotope effect for acrolein formation. The initial isotope effect published previously was 1/0.55 for Bi—Mo oxide at 450°C (*17*), 0.48 for U–Sb oxide at 400°C (*18*), and 0.55 for Sb–Sn oxide at 400°C (*6*), indicating that the allylic hydrogen abstraction is rate determining. The results for Sb (18)–Ti–O as well as for Sb_6O_{13} also suggest that the first hydrogen abstraction step is rate determining. The amounts of CH_2=CH—CDO and CD_2=CH—CHO were nearly equal and indicate that the second H(D) abstraction occurs with little or no isotope effect.

In order to obtain more complete information on the second hydrogen abstraction, the oxidation of *cis*-CHD=CD—CH_3 was studied. The formation of π-allyl intermediate (CHD···CD···CH_2) should lead to four acrolein species (Table 5). The results over $Sb_6O_{13}$and Sb(18)–Ti–O catalysts gave ratios for ACR-1,2-d_2 : ACR-2-d_1 : ACR-*trans*-2,3-d_2 : ACR-*cis*-2,3-d_2 = 1.1–1.2 : 1 : 1 : 1. These species are produced at nearly equal probability; consistent with the results with CH_2=CH—CD_3 + CH_2=CH—CH_3, there exist little or no isotope effects in the secondary hydrogen abstraction. A similar situation was observed in the case of unsupported Rh catalysts as reported by Imachi *et al.* (*12*). They have discussed reasons for this observation including one possibility which involves a less symmetric surface π-allyl intermediate (*12*). The results for Sb_6O_{13} and Sb(18)–Ti–O are almost the same. This indicates that the reaction scheme for propene oxidation over Sb (18)–Ti–O is the same as that on Sb_6O_{13}. A small excess in the amount of ACR-1,2-d_2 appears evident. This may be due in part to the deuterium substitution at the aldehyde in ACR-1,2-d_2 and an isotope effect at this site in some subsequent oxidation of acrolein. It may also indicate that the second H-abstraction from the CHD-end of the allyl species occurs faster than from the CH_2-end. Such a special isotope effect has been observed by Amenomiya and Pottie (*20*) who reported that the loss of H and D from deuterated ethanes in their mass spectrometric fragmentation depends on the amount of deuterium in the ethane; i.e., the loss of H increases with D substitution.

TABLE 5

Relative Acrolein Formation Rates in the Oxidation of *cis*-CHD=CD—CH_3 over Two Catalysts[a]

	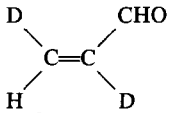 (ACR-*trans*-2,3-d_2)	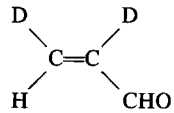 (ACR-*cis*-2,3-d_2)	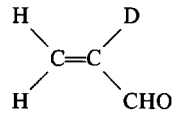 (ACR-2-d_1)	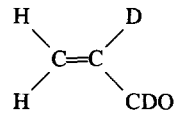 (ACR-1,2-d_2)
Sb(18)–Ti–O	1.00	1.01	0.99	1.19
Sb_6O_{13}	1.00	0.99	0.97	1.13

[a] Experimental conditions: temperature 400°C, *cis*-CHD=CD—CH_3 (99%) = 15 Torr, P_{O_2} = 31 Torr, propene conversion 5%, acrolein selectivity ca. 70%.

Kinetics of propene oxidation. As described above, Sb_6O_{13}, Sb(18)–, and Sb (55)–Ti–O have nearly the same selectivities to acrolein and CO + CO_2, suggesting that the rate constants for the propene oxidation can be inferred by using a redox mechanism.

As has been proposed by a number of workers, for example, with Bi–Mo oxides (*3, 19*), the reduction of the oxides with propene and its oxidation by gaseous oxygen occur in different regions on the surface, A and B, respectively. The surface anion vacancies formed in region A are refilled by diffusion of the oxide ions in the bulk, which results in the formation of surface anion vacancies in region B. These vacancies bring about the oxygen uptake. Assuming the stationary state of the oxygen flow ($-d[O]_A/dt = d[O]_B/dt$, where [O] denotes the surface oxygen concentration at each region), the following equation holds (*21*):

$$k_A N_A P_{C_3H_6} \Theta_A = k_B N_B P_{O_2}^{1/2}(1 - \Theta_B), \quad (1)$$

where Θ and $1 - \Theta$ refer to the fraction of the surface oxygen and anion vacancies in regions A and B, respectively. N_A and N_B are the maximum surface oxygen concentrations which participate in the oxidation. k_A and k_B are the rate constants for the reduction step in region A and for the reoxidation step in region B, respectively. A similar situation will be applicable to the Sb–Ti–O catalysts. There appears to be no marked difference between values of Θ_A and Θ_B ($\simeq\Theta$), if the diffusion of the oxide ions from region B to A is very rapid as compared to the surface reduction. Accordingly, the above equation is transformed as

$$k_1 P_{C_3H_6}\Theta = k_2 P_{O_2}^{1/2}(1 - \Theta),$$

where k_1 ($=k_A N_A$) is the rate constant for the reduction step and k_2 ($=k_B N_B$) for the reoxidation step. The following rate equation results, which is similar to that from a simple redox model:

$$R = k_1 k_2 P_{C_3H_6} P_{O_2}^{1/2}/(k_1 P_{C_3H_6} + k_2 P_{O_2}^{1/2}).$$

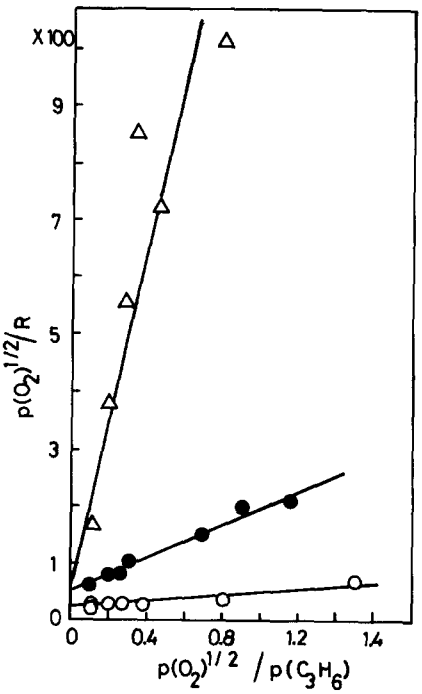

FIG. 3. Plots of $P_{O_2}^{1/2}/R$ vs $P_{O_2}^{1/2}/P_{C_3H_6}$ for Sb_6O_{13} (△), Sb(18)–Ti–O (○), and Sb(55)–Ti–O (●). The slope and intercept give $1/k_1$ and $1/k_2$, respectively.

Using this equation, the rate constants for the catalysts are calculated by applying the data in the range from 6 to 60 Torr of propene and oxygen (Fig. 3 and Table 6). As shown in Fig. 3, the plots lie on straight lines with each catalyst. This is consistent with Eq. (1). With Sb_6O_{13}, k_2/k_1 is 22, indicating that the reduction step is rate determining.

TABLE 6

Rate Constants in the Oxidation of Propene over the Catalysts at 400°C

Catalyst (Sb at.%)	Rate constants[a]		
	k_1	k_2	k_2/k_1
Sb_6O_{13}	0.063×10^{-2}	1.4×10^{-2}	22
Sb(18)–Ti–O	3.1×10^{-2}	4.5×10^{-2}	1.5
Sb(55)–Ti–O	0.7×10^{-2}	1.8×10^{-2}	2.5

[a] Calculated from the equation $R = k_1 k_2 P_{C_3H_6} P_{O_2}^{1/2}/(k_1 P_{C_3H_6} + k_2 P_{O_2}^{1/2})$, see text; R is rate in μmol/min m^2 (C_3H_6 reacted). Pressure ranges: $P_{C_3H_6}$ = 6–60 Torr and P_{O_2} = 6–60 Torr (1 Torr = 133 Pa).

With Sb(18)– and Sb(55)–Ti–O catalysts, k_2/k_1 values are 1–2. This suggests that the reduction and reoxidation steps have comparable rates. Comparison between Sb_6O_{13} and Sb(18)–Ti–O catalysts shows that the reduction step is promoted by a factor of 50, while the reoxidation step is not promoted so much. If both the reduction and reoxidation sites increase on the TiO_2 support, the ratio k_2/k_1 would not change between Sb_6O_{13} and Sb(18)Ti–O. However, they change significantly. As found by labeled propene studies, the isotope effect for the first hydrogen abstraction on the Sb(18)–Ti–O catalyst is a little larger than that on Sb_6O_{13}. Thus, there does not seem to be a large difference in the nature of first hydrogen abstraction between Sb_6O_{13} and Sb(18), (55)–Ti–O. Therefore, the rate promotion in the reduction step seems to originate from the increase in the number of the active sites (N_A) rather than in the k_A of Eq. (1).

As reported previously, with the V–Ti–O and Mo–Ti–O catalysts (*9*), the reduction step (k_1) in the propene oxidation over V oxide or Mo oxide dispersed on TiO_2 was also enhanced, while the reoxidation step (k_2) was not. Similar results were also obtained in the case of Mo oxide dispersed on ZrO_2 (*10*) and V–Mo mixed oxide catalysts (*21*). The same analysis as described above would be applicable in these cases.

In the case of Sb–Sn oxide catalysts, Volta *et al.* (*4*) have proposed that the surface Sb^{3+}–Sb^{5+} couples produced on SnO_2 into which Sb ions are dissolved should be responsible for partial oxidation. We have proposed (*5, 6*) that the promotion of the oxidation activity can be attributed to an increase in the reduction step due to the presence of Sn ions. With U–Sb oxide catalysts, Grasselli *et al.* (*3*) have proposed the following:

$$C_3H_6 \xrightarrow{Sb^{3+}\text{–O–}Sb^{5+}} \pi\text{-allyl}$$

$$\pi\text{-allyl} \xrightarrow{Sb^{5+}\text{–O–}Sb^{5+}} CH_2{=}CH{-}CHO$$

They explained that the Sb^{3+}–O–Sb^{5+} and Sb^{5+}–O–Sb^{5+} moieties are responsible for π-allyl formation and oxygen insertion during acrolein formation, respectively.

In the present work, as described above, Sb ions do not seem to dissolve into the TiO_2 lattice and the Sb(5.5)–Ti–O catalyst has a higher concentration of Sb^{3+} than others, but there is no strong evidence that the Sb(18)– and Sb(55)–Ti–O catalysts have an excess of Sb^{3+} on the surface. The IR, Auger, and XRD results indicate that electronic environment around Sb is perturbed in the low Sb content catalysts, perhaps suggesting that the Sb oxide is somewhat distorted as compared to Sb_6O_{13}. In that case the increase in the reduction sites might be attributed to the exposure of Sb^{3+} ions by the interaction with TiO_2 which affects a change in coordination geometry around Sb.

ACKNOWLEDGMENTS

The authors thank Dr. Takashi Ohno (Kobe University) for FTIR measurements, Dr. Kurt Hillig for assistance in the isotope labeling experiments, and the Rackham Graduate School at the University of Michigan for supplies and equipment funds. The microwave spectrometer was supported by a grant from the National Science Foundation, Washington, DC.

REFERENCES

1. Berry, F. J., *in* "Advances in Catalysis" (D. D. Eley, H. Pines, and P. B. Weisz, Eds.), Vol. 30, p. 97. Academic Press, New York, 1981.
2. Centi, G., and Trifiro F., *Catal. Rev.* **28,** 165 (1986).
3. Grasselli, R. K., Brazdil, J. F., and Burrington, J. D., *in* "Proceedings, 8th International Congress on Catalysis, Berlin, 1984," Vol. V, p. 369. Dechema, Frankfurt-am-Main, 1984; Burrington, J. D., Kartisek, C. T., and Grasselli, R. K., *J. Catal.* **87,** 363 (1984).
4. Volta, J. C., Bussiere, P., Coudurier, G., Herrmann, J. M., and Vedrine, J. C., *Appl. Catal.* **16,** 315 (1985).
5. Ono, T., Yamanaka, T., Kubokawa, Y., and Komiyama, M., *J. Catal.* **109,** 423 (1988).
6. Ono, T., Hillig, K. W., II, and Kuczkowski, R. L., *J. Catal.* **123,** 236 (1990).
7. For example, Haller, G. L. and Resasco, D. E., *in* "Advances in Catalysis" (D. D. Eley, H. Pines, and P. B. Weisz, Eds.), Vol. 36, p. 173. Academic Press, New York, 1989.

8. For example, Bond, G. C., Zurita, J. P., and Framerz, S., *Appl. Catal.* **22,** 361 (1986); Miyamoto, M., Yamazaki, Y., Inomata, M., and Murakami, Y., *J. Phys. Chem.* **85,** 2368, 2377 (1981); Gavani, F., Genti, G., Foresti, E., Trifiro, F., and Busca, G., *J. Catal.* **106,** 251 (1987); Haber, J., Kozlowska, A., and Kozlowski, R., *J. Catal.* **102,** 52 (1986); Kang, Z. C., and Bao, Q. X., *Appl. Catal.* **26,** 251 (1986).
9. Ono, T., Nakagawa, Y., Miyata, H., and Kubokawa, Y., *Bull. Chem. Soc. Japan* **57,** 1205 (1984).
10. Ono, T., Miyata, H., and Kubokawa, Y., *J. Chem. Soc. Faraday Trans. 1* **83,** 1761 (1987).
11. Imachi, M., Cant, N. W., and Kuczkowski, R. L., *J. Catal.* **75,** 404 (1982).
12. Imachi, M., Kuczkowski, R. L., Groves, J. T., and Cant, N. W., *J. Catal.* **82,** 355 (1983).
13. Choi, H., Lin, J., and Kuczkowski, R. L., *J. Catal.* **99,** 72 (1986).
14. Sala, F., and Trifiro, F., *J. Catal.* **41,** 1 (1976).
15. Komiyama, M., Yoshii, M., Ogino, Y., and Ono, T., *Shokubai* **29,** 498 (1987). [Japanese]
16. Zenkovets, G. A., Tarasova, D. V., Andrushkevich, T. V., Aleshina, G. I., Nikoro, T. A., and Ravirov, R. G., *Kinet. Catal.* **20,** 307 (1979).
17. Adams, C. R., and Jennings, T. J., *J. Catal.* **3,** 549 (1964).
18. Keulks, G. W., Yu, Z., and Krenzke, L. D., *J. Catal.* **84,** 38 (1983).
19. For example, Matsuura, I., and Schuit G. C. A., *J. Catal.* **25,** 314 (1972); Haber, J., and Grzybowska, J., *J. Catal.* **28,** 489 (1973); Otsubo, T., Miura, H., Morikawa, Y., and Shirasaki, T., *J. Catal.* **36,** 240 (1975); Ueda, W., Moro-Oka, Y., and Ikawa, T., *J. Chem. Soc. Faraday Trans. 1* **78,** 495 (1982).
20. Amenomiya, Y., and Pottie, R. F., *Canad. J. Chem.* **46,** 1741 (1968).
21. Ono, T., and Kubokawa, Y., *Bull. Chem. Soc. Japan,* **55,** 1748 (1982).